Available online at www.sciencedirect.com

ScienceDirect

Nuclear and Particle Physics Proceedings 267–269 (2015) 294–301

www.elsevier.com/locate/nppp

CP-Violation in Top Quark Pair Production in the Complex MSSM at Hadron Colliders

S. Berge[a], M. Mühlleitner[b], A. Moreno Briceño[c], D. Wackeroth[d], M. Wiebusch[e]

[a]*Institute for Theoretical Physics, RWTH Aachen University, 52056 Aachen, Germany*
[b]*Institute for Theoretical Particle Physics, Karlsruhe Institute of Technology (KIT)), D-76128 Karlsruhe, Germany*
[c]*Centro de Investigaciones en Ciencias Básicas y Aplicadas, Universidad Antonio Nariño, Cra. 3 Este No. 47A-15, Bogotá, Colombia*
[d]*Department of Physics, University at Buffalo, The State University of New York, Buffalo, NY 14260-1500, USA*
[e]*Institute for Particle Physics Phenomenology, Department of Physics, Durham University, Durham CH1 3LE, United Kingdom*

Abstract

We study possible CP violating effects due to the one loop corrections to the top quark pair production in the Complex MSSM with minimal flavor violation (MFV) at hadron colliders. We calculate the complete SUSY Electroweak and SUSY QCD corrections to the two main production mechanisms, namely: the quark-antiquark annihilation and the gluon fusion processes. At the top quark level, we study the spin-spin correlating observables that may be sensitive to the CP violating phases presented in the Complex MFV-MSSM. We present here the main results at the parton level, in particular the SUSY QCD contributions, which are the most important ones.

Keywords: CP-violation, Spin-correlations, top quark, MSSM, LHC, hadron collider physics

1. Introduction

The study of top quark properties and dynamics provides a very unique and interesting window to the Standard Model (SM) itself and to the study of physics beyond the SM (BSM). Due to its large mass, which is at the electroweak symmetry breaking (EWSB) scale, it plays a very important role in the study of the mechanism of EWSB and also in searching for signals of new physics (NP) connected to EWSB, which may be found through precision studies of top quark observables [1, 2]. Deviations of experimental measurements from SM predictions, including electroweak (EW) and QCD corrections, could show non-standard top quark production or decay mechanisms [2]. The top quark has a very short lifetime, smaller than its hadronization time, which means that it decays before it hadronizes or flips its spin [1, 2]. This provides a very interesting testing ground for perturbative QCD. In addition, information about spin correlation and polarization coming from the top-pair production processes are conserved during their decay and can be studied in angular distributions of top decay products. This provides another interesting way of searching for deviations from SM expectations [1, 2]. Searches for non-SM signals in top quark pair production asymmetries, such as the forward-backward asymmetry, observed at the Tevatron [3], parity violating asymmetries in polarized top pair quark production [4] and spin correlation between t and $\bar{t}$ [5, 6, 7, 8, 9, 10], require the inclusion of radiative corrections to top production and decay [2].

Supersymmetry [11, 12] is one of the most natural and appealing concepts of physics BSM, although no direct or indirect experimental evidence has been observed so far. It is an experimental fact that supersymmetry must be broken, otherwise we would have found

Email addresses: berge@physik.rwth-aachen.de (S. Berge), maggie@particle.uni-karlsruhe.de (M. Mühlleitner), alexander.moreno@uan.edu.co (A. Moreno Briceño), dow@ubpheno.physics.buffalo.edu (D. Wackeroth), martin.wiebusch@durham.ac.uk (M. Wiebusch)

http://dx.doi.org/10.1016/j.nuclphysbps.2015.10.121

evidence for supersymmetric particles already. Since we do not know the dynamics of the supersymmetric breaking mechanism, we have to explicitly break supersymmetry by introducing mass terms for the supersymmetric partners of the SM particles. This must be done in such a way that we do not reintroduce any fine-tuning in the theory, and we can do it through the so called soft-supersymmetric breaking term. This term introduces more than 100 new free parameters, such as couplings, mixing angles and phases, which can be in general complex. Complex phases in the MSSM can be possible sources of CP violation. In the SM there is only one complex phase which is the source of CP violation and which comes from the Cabibbo-Kobayashi-Maskawa (CKM) mixing matrix, but the amount predicted and observed in K, B and D meson systems is not enough to explain the Baryon Asymmetry of the Universe (BAU). So we need to look for new phases that can be sources of CP violation, and the Complex MSSM provides an interesting scenario which contains new complex phases responsible for CP violation.

We study possible CP violating effects due to one loop corrections to top-quark pair production at the Large Hadron Collider (LHC) in the context of the Complex MSSM with minimal flavor violation (MFV). We include the complete supersymmetric QCD as well as supersymmetric electroweak contributions to the top-quark pair production mechanisms, namely quark-antiquark annihilation, $q\bar{q} \to t\bar{t}$, and gluon fusion, $gg \to t\bar{t}$. At the level of the top quarks, we study in detail spin-spin correlating observables that are sensitive to CP violating phases of the Complex MFV-MSSM. We present results for these observables at the parton level, where we show the maximal possible contributions of the one loop MSSM corrections.

In section 2 we will introduce the MSSM with complex parameters with minimal flavor violation, the Complex MFV-MSSM, and will study the complex parameters in the soft-supersymmetry breaking term. We will discuss which phases can lead to CP violating effects in interactions involving supersymmetric particles. We will present in section 3 the top quark pair production at LO in QCD and NLO and the top quark pair production density matrix which will allow us to study two spin-spin correlating observables that may be sensitive to the CP violating phases of the Complex MVF-MSSM. In section 4 we study the possible CP violating effects due to one loop corrections to top-quark pair production at the LHC in the Complex MFV-MSSM. At the level of the top quarks, we study in detail spin-spin correlating observables that are sensitive to CP violating phases of the Complex MFV-MSSM. We present the main results for these observables at the parton level, where we show the maximal possible contributions of the one loop MSSM corrections. Finally, in section 5 we conclude.

2. The Complex Minimal Supersymmetric Standard Model with Minimal Flavor Violation (MFV-MSSM)

The complex minimal supersymmetric extension of the SM with minimal flavor violation (MFV-MSSM) [13, 14] is determined by the gauge group, the particle content, the non-gauge interactions and the soft-SUSY breaking terms. The possible complex phases appear in the complex parameters of the soft-SUSY breaking terms. In this section we present the complex phases of these terms which can be possible sources of CP violation, in addition to the source of CP violation in the SM, that come from the complex phase of the CKM mixing matrix.

2.1. The Soft Supersymmetry Breaking Term

Supersymmetry is not an exact symmetry, which means that the superpartners of the SM particles have different masses. Since we do not know how exactly supersymmetry is broken, we have to break explicitly supersymmetry by introducing terms that break supersymmetry and at the same time do not reintroduce quadratic divergences. This is done by adding the so-called soft supersymmetry-breaking terms to the Lagrangian density:

- Mass terms for the gluinos, winos and binos:

$$-\mathscr{L}_{gaugino} = \frac{1}{2}\Big[M_1\tilde{B}\tilde{B} + M_2\sum_{a=1}^{3}\tilde{W}^a\tilde{W}_a + M_3\sum_{a=1}^{8}\tilde{G}^a\tilde{G}_a + \text{h.c.}\Big]. \quad (1)$$

- Mass terms for the scalar fermions:

$$-\mathscr{L}_{sfermions} = \sum_{i=gen} m^2_{\tilde{Q}_i}\tilde{Q}_i^\dagger\tilde{Q}_i + m^2_{\tilde{L}_i}\tilde{L}_i^\dagger\tilde{L}_i + m^2_{\tilde{u}_i}|\tilde{u}_{Ri}|^2 + m^2_{\tilde{d}_i}|\tilde{d}_{Ri}|^2 + m^2_{\tilde{l}_i}|\tilde{l}_{Ri}|^2. \quad (2)$$

- Mass and bilinear terms for the Higgs bosons:

$$-\mathscr{L}_{Higgs} = m_{H_2}^2 H_2^\dagger H_2 + m_{H_1}^2 H_1^\dagger H_1 + B\mu(H_2 \cdot H_1 + \text{h.c.}). \quad (3)$$

- Trilinear couplings between sfermions and Higgs bosons:

$$-\mathscr{L}_{tril.} = \sum_{i,j=gen} \Big[A_{ij}^u Y_{ij}^u \tilde{u}_{Ri}^\star H_2 \cdot \tilde{Q}_j + A_{ij}^d Y_{ij}^d \tilde{d}_{Ri}^\star H_1 \cdot \tilde{Q}_j + A_{ij}^l Y_{ij}^l \tilde{l}_{Ri}^\star H_1 \cdot \tilde{L}_j + \text{h.c.} \Big]. \quad (4)$$

The soft supersymmetry-breaking scalar potential is the sum of the three last terms:

$$V_{soft} = -\mathscr{L}_{sfermions} - \mathscr{L}_{Higgs} - \mathscr{L}_{tril.}. \quad (5)$$

The general form of the minimal supersymmetric extension of the standard model allows complex parameters such as the binos and winos mass terms (M_1, M_2), the gluino mass term (M_3), the bilinear Higgs term (μ), and the trilinear coupling (A^f). The phases of these complex parameters can induce CP violating effects in interactions involving SUSY particles.

2.2. The Scalar Quark Sector

The superpartners of the left and right-handed quarks are the left and right-handed scalar quarks, $\tilde{q}_L$ and $\tilde{q}_R$. The part of the Complex MFV-MSSM density Lagrangian that contains the squark mass terms is given by [15]

$$\mathscr{L} = -\begin{pmatrix} \tilde{q}_L^* & \tilde{q}_R^* \end{pmatrix} \mathscr{M}_{\tilde{q}} \begin{pmatrix} \tilde{q}_L \\ \tilde{q}_R \end{pmatrix} \quad (6)$$

with

$$\mathscr{M}_{\tilde{q}} = \begin{pmatrix} M_L & m_q X_q^* \\ m_q X_q & M_R \end{pmatrix}, \quad (7)$$

where $M_L = M_{\tilde{q}_L}^2 + m_q^2 + M_Z^2 \cos 2\beta (I_3^q - Q_q s_W^2)$, $M_R = M_{\tilde{q}_R}^2 + m_q^2 + M_Z^2 \cos 2\beta Q_q s_W^2$ and $X_q = A_q - \mu^\star \cot\beta (\tan\beta)$ ($\cot\beta$ for up-type quarks and $\tan\beta$ for down-type quarks). $M_{\tilde{q}_L}^2$ and $M_{\tilde{q}_R}^2$ are real soft-supersymmetry breaking squark-mass parameters, and the trilinear coupling A_q and the bilinear Higgs coupling μ are complex parameters. Thus we have $N_q + 1$ new free parameters, N_q from each trilinear coupling A_q and one from μ. $\tilde{q}_L$ and $\tilde{q}_R$ are not necessarily mass eigenstates, since $\mathscr{M}_{\tilde{q}}$ is of non-diagonal form [15]. Thus, $\tilde{q}_L$ and $\tilde{q}_R$ can mix, so that the physical mass eigenstates $\tilde{q}_1$ and $\tilde{q}_2$ are model-dependent linear combinations of these states. The latter are obtained by diagonalizing the mass matrix performing the transformation [15]

$$\begin{pmatrix} \tilde{q}_1 \\ \tilde{q}_2 \end{pmatrix} = \mathbf{U}_{\tilde{\mathbf{q}}} \begin{pmatrix} \tilde{q}_L \\ \tilde{q}_R \end{pmatrix}, \quad (8)$$

where

$$\mathbf{U}_{\tilde{\mathbf{q}}} = \begin{pmatrix} c_{\tilde{q}} & s_{\tilde{q}} \\ -s_{\tilde{q}} & c_{\tilde{q}} \end{pmatrix} \quad (9)$$

and $\mathbf{U}_{\tilde{\mathbf{q}}} \mathbf{U}_{\tilde{\mathbf{q}}}^\dagger = 1$. The elements of the mixing matrix $\mathbf{U}$ are [15]

$$c_{\tilde{q}} = \frac{\sqrt{M_L - m_{\tilde{q}_2}^2}}{\sqrt{m_{\tilde{q}_1}^2 - m_{\tilde{q}_2}^2}}, \quad (10)$$

$$s_{\tilde{q}} = \frac{m_q X_q^\star}{\sqrt{M_L - m_{\tilde{q}_2}^2}\sqrt{m_{\tilde{q}_1}^2 - m_{\tilde{q}_2}^2}}. \quad (11)$$

$c_{\tilde{q}} \equiv \cos\theta_{\tilde{q}}$ is real and $s_{\tilde{q}} \equiv \exp(-i\phi X_q)\sin\theta_{\tilde{q}}$ can be complex. The mass eigenvalues are independent of any complex phase and are given by [15]

$$m_{\tilde{q}_{1,2}}^2 = m_q^2 + \frac{1}{2}\Big[M_{\tilde{q}_L}^2 + M_{\tilde{q}_R}^2 + I_3^q M_Z^2 \cos 2\beta \mp \sqrt{[M_{LR}]^2 + 4m_q^2 |X_q|^2} \Big] \quad (12)$$

with $M_{LR} = M_{\tilde{q}_L}^2 - M_{\tilde{q}_R}^2 + M_Z^2 \cos 2\beta (I_3^q - 2Q_q s_W^2)$.

2.3. The Chargino and Neutralino Sector

The part of the Complex MFV-MSSM Lagrangian density that contains the chargino mass terms is given by

$$\mathscr{L} = -\begin{pmatrix} \tilde{\chi}_1 & \tilde{\chi}_2 \end{pmatrix} \mathbf{X} \begin{pmatrix} \tilde{\chi}_1 \\ \tilde{\chi}_2 \end{pmatrix} \quad (13)$$

with [15]

$$\mathbf{X} = \begin{pmatrix} M_2 & \sqrt{2}\sin\beta M_W \\ \sqrt{2}\cos\beta M_W & \mu \end{pmatrix}, \quad (14)$$

where μ and M_2 can be complex. In order to get the mass eigenstates of the charginos, the wino and higgsino fields must be rotated by two unitary matrices $\mathbf{V}$ and $\mathbf{U}$ [15],

$$\begin{pmatrix} \tilde{\chi}_1^+ \\ \tilde{\chi}_2^+ \end{pmatrix} = \mathbf{V} \begin{pmatrix} \tilde{W}^+ \\ \tilde{H}_2^+ \end{pmatrix} \quad (15)$$

and

$$\begin{pmatrix} \tilde{\chi}_1^- \\ \tilde{\chi}_2^- \end{pmatrix} = \mathbf{U} \begin{pmatrix} \tilde{W}^- \\ \tilde{H}_1^- \end{pmatrix}. \quad (16)$$

These two matrices lead to [15]

$$\begin{pmatrix} m_{\tilde{\chi}_1^\pm} & 0 \\ 0 & m_{\tilde{\chi}_2^\pm} \end{pmatrix} = \mathbf{U}^* \mathbf{X} \mathbf{V}^\dagger. \quad (17)$$

As for the neutralino sector, the Lagrangian reads

$$\mathscr{L} = -\left(\tilde{\chi}_1^0 \quad \tilde{\chi}_2^0 \quad \tilde{\chi}_3^0 \quad \tilde{\chi}_4^0 \right) \mathbf{Y} \begin{pmatrix} \tilde{\chi}_1^0 \\ \tilde{\chi}_2^0 \\ \tilde{\chi}_3^0 \\ \tilde{\chi}_4^0 \end{pmatrix} \quad (18)$$

where [15]

$$\mathbf{Y} = \begin{pmatrix} M_1 & 0 & -Msc & Mss \\ 0 & M_2 & Mcc & Mcs \\ -Msc & Mcc & 0 & -\mu \\ Mss & Mcs & -\mu & 0 \end{pmatrix}, \quad (19)$$

where $Msc = M_Z s_W \cos\beta$, $Mss = M_Z s_W \sin\beta$, $Mcc = M_Z c_W W \cos\beta$ and $Mcs = M_Z c_W \sin\beta$.

In this sector we have the additional mass term, M_1, which can be complex. In order to get the neutralino masses, the bino, wino and higgsino fields must be rotated by the matrix **N** [15],

$$\begin{pmatrix} \tilde{\chi}_1^0 \\ \tilde{\chi}_2^0 \\ \tilde{\chi}_3^0 \\ \tilde{\chi}_4^0 \end{pmatrix} = \mathbf{N} \begin{pmatrix} \tilde{B}^0 \\ \tilde{W}^0 \\ \tilde{H}_1^0 \\ \tilde{H}_2^0 \end{pmatrix} \quad (20)$$

and [15]

$$\mathbf{N}^* \mathbf{Y} \mathbf{N}^\dagger = \begin{pmatrix} m_{\tilde{\chi}_1^0} & 0 & 0 & 0 \\ 0 & m_{\tilde{\chi}_2^0} & 0 & 0 \\ 0 & 0 & m_{\tilde{\chi}_3^0} & 0 \\ 0 & 0 & 0 & m_{\tilde{\chi}_4^0} \end{pmatrix}. \quad (21)$$

In the next section we will introduce a top quark pair production density matrix at NLO which will allow us to define two CP violating observables which are sensitive to the complex phases of the Complex MFV-MSSM.

3. Top Quark Pair Production and Density Matrix

3.1. Top Quark Pair Production at LO in QCD and NLO

At leading order (LO) in QCD, the partonic cross section for top quark pair production at hadron colliders is of order $O(\alpha_s^2)$, the subprocesses that contribute to the cross section at this level are the quark-antiquark annihilation and the gluon-gluon fusion processes:

$$\begin{aligned} q(p_1)\bar{q}(p_2) &\rightarrow t(k_1,s_1) + \bar{t}(k_2,s_2) \\ g(p_1)g(p_2) &\rightarrow t(k_1,s_1) + \bar{t}(k_2,s_2), \end{aligned} \quad (22)$$

where p_1, p_2 (k_1, k_2) are the momenta of the initial (final top) particles and s_1 (s_2) are the spin 4-vectors of the top (antitop) quark.

The partonic differential cross section to the quark-antiquark annihilation and gluon-gluon fusion processes at NLO SUSY EW and SUSY QCD is given by

$$\begin{aligned} d\hat{\sigma}_{q\bar{q},gg} &= d\hat{\sigma}^{LO}_{q\bar{q},gg} + \delta d\hat{\sigma}_{q\bar{q},gg} \\ &= \frac{d\Phi_{2\to 2}}{8\pi^2 \hat{s}} \Big[\overline{\sum} |\mathscr{M}_B^{q\bar{q},gg}|^2 + \\ &\quad 2Re\overline{\sum}(\delta\mathscr{M}_{q\bar{q},gg}^{SUSYEW} \times \mathscr{M}_B^{q\bar{q},gg}) + \\ &\quad 2Re\overline{\sum}(\delta\mathscr{M}_{q\bar{q},gg}^{SQCD} \times \mathscr{M}_B^{q\bar{q},gg}) \Big], \end{aligned} \quad (23)$$

where $d\Phi_{2\to 2}$ denotes the 2-particle phase space factor and $\hat{s} = (p_1 + p_2)^2$ is the partonic center of mass energy. $\overline{\sum}|\mathscr{M}_B^{q\bar{q},gg}|^2$ denotes the color and spin averaged squared matrix element given by $\overline{\sum}|M|^2 = \frac{1}{4} \cdot \frac{1}{N} \cdot |M|^2$ with $N := N_{\{q\bar{q},gg\}} = \{9, 64\}$.

3.2. Top Quark Pair Production Density Matrix

We can express the partonic cross section for the quark-antiquark annihilation and gluon-gluon fusion processes in terms of a density matrix [16]

$$\begin{aligned} R(\vec{p},\vec{k}) = \frac{1}{N} \sum & \langle t(k_1,\alpha_1), \bar{t}(k_2,\beta_1) | T | a(p_1)\bar{a}(p_2) \rangle^* \\ & \langle t(k_1,\alpha_2), \bar{t}(k_2,\beta_2) | T | a(p_1)\bar{a}(p_2) \rangle \end{aligned} \quad (24)$$

with the top spin index α and the antitop spin index β. The sum runs over the spin and color of all initial and state final particles. For convenience we denote the vectors (normalized vectors) by $\vec{p} := \vec{p}_1$ ($\hat{p} = \hat{\vec{p}}_1$) and $\vec{k} := \vec{k}_1$ ($\hat{k} := \hat{\vec{k}}_1$). The density matrix R can be decomposed in the top and antitop spin space as [16]

$$R = A \cdot \mathbf{1} \otimes \mathbf{1} + \vec{B}^+ \cdot \vec{\sigma} \otimes \mathbf{1} + \mathbf{1} \otimes \vec{\sigma} \cdot \vec{B}^- + C_{ij}\, \sigma_i \otimes \sigma_j \quad (25)$$

with

$$B_i^{\pm} = b_1^{\pm}\hat{p}_i + b_2^{\pm}\hat{k}_i + b_3^{\pm}\hat{n}_i \quad (26)$$

$$C_{ij} = c_0\,\delta_{ij} + \varepsilon_{ijl}\left(c_1\hat{p}_l + c_2\hat{k}_l + c_3\hat{n}_l\right) + c_4\hat{p}_i\hat{p}_j + c_5\hat{k}_i\hat{k}_j + c_6\left(\hat{p}_i\hat{k}_j + \hat{p}_j\hat{k}_i\right) + c_7\left(\hat{p}_i\hat{n}_j + \hat{n}_i\hat{p}_j\right) + c_8\left(\hat{k}_i\hat{n}_j + \hat{n}_i\hat{k}_j\right), \quad (27)$$

where $\{i,j\} = 1,2,3$ and $\vec{n} = \vec{p}\times\vec{k}$. The first factor of the tensor product of the 2×2 unit matrices $\mathbf{1}$ and the Pauli matrices $\vec{\sigma}$ in Eq. (25) refers to top spin space, the second factor of the tensor product refers to the antitop spin space. The structure functions $A, b_i^{\pm}, c_i$ depend only on the partonic center of mass energy $\hat{s}$ and on the cosine of the scattering angle $z = \cos\theta_t = \hat{p}\hat{k}$.

The contributions to the density matrix R can be decomposed into a CP-even and a CP-odd part:

$$R = R_{CP-even} + R_{CP-odd}. \quad (28)$$

We have that the CP-odd part of the density matrix R is:

$$R_{CP-odd} = (b_1^{CP-odd}\hat{p}_i + b_2^{CP-odd}\hat{k}_i + b_3^{CP-odd}\hat{n}_i)(\sigma^i\otimes\mathbf{1} - 1\otimes\sigma^i) + \varepsilon_{ijk}(c_1\hat{p}_i + c_2\hat{k}_i + c_3\hat{n}_i)\sigma_j\otimes\sigma_k. \quad (29)$$

Interactions with CP violation, which are also parity violating, can give contributions to b_1^{CP-odd}, b_2^{CP-odd}, c_1 and c_2. Nonzero b_1^{CP-odd} and b_2^{CP-odd} require in addition absorptive parts.

The density matrix R is related to the averaged squared matrix element by

$$\left|\overline{M}(\vec{s}_1,\vec{s}_2)\right|^2 = Tr\left[R\cdot\frac{1}{2}(\mathbf{1}+\vec{s}_1\vec{\sigma})\otimes\frac{1}{2}(\mathbf{1}+\vec{s}_2\vec{\sigma})\right], \quad (30)$$

where $\vec{s}_1$ ($\vec{s}_2$) is the normalized top (antitop) quark spin vector in the top (antitop) quark's rest frame. To extract the coefficients A, $b_i^{\pm}$ and c_i of Eq. (25), (26) and (27) one calculates $\left|\overline{M}(\vec{s}_1,\vec{s}_2)\right|^2$ in the $q\bar{q}, gg$ parton CMS and then has to boost the top and antitop spin vectors from the parton CMS to the appropriate top (antitop) rest frame via

$$\overline{|M(\vec{s}_1,\vec{s}_2)|}^2 = A + \left(\vec{B}^{+}\cdot\vec{s}_1\right) + \left(\vec{B}^{-}\cdot\vec{s}_2\right) + C_{ij}\left(s_{1i}s_{2j}\right). \quad (31)$$

From eq. (31) we can now extract the coefficient functions of the density matrix R.

3.3. CP Violating Observables

We define spin correlation observables at the top quark level by using the top production density matrix of subsection 3.2. The expectation value of an observable $\mathcal{O}$ is defined by [16]

$$\langle\mathcal{O}\rangle = \frac{\int_{-1}^{1} dz\, Tr(R\,\mathcal{O})}{4\int_{-1}^{1} dz A}. \quad (32)$$

We define the expectation values of the CP violating observables as

1. $\langle\mathcal{O}_1\rangle := \left\langle\hat{k}\cdot(\vec{s}_1 - \vec{s}_2)\right\rangle$,
2. $\langle\mathcal{O}_2\rangle := \left\langle\hat{k}\cdot(\vec{s}_1\times\vec{s}_2)\right\rangle$.

The first expectation value, $\langle\mathcal{O}_1\rangle$, corresponds to the known helicity asymmetry

$$A_1^{t\bar{t}} = \frac{\sigma(++) - \sigma(--)}{\sigma_{tot}}. \quad (33)$$

The expectation value of $\left\langle\hat{k}\cdot(\vec{s}_1 - \vec{s}_2)\right\rangle$ receives contributions of b_1^{CP} and b_2^{CP}, which come from the $CP-odd$ part of the density matrix R, and is given by

$$\langle\mathcal{O}_1\rangle = \left\langle\hat{k}\cdot(\vec{s}_1 - \vec{s}_2)\right\rangle = \frac{4\int_{-1}^{1} dz\left(z\cdot b_1^{CP} + b_2^{CP}\right)}{4\int_{-1}^{1} dz A}. \quad (34)$$

Non-zero values of b_1^{CP} and b_2^{CP} require an absorptive part in addition to a CP-violating interaction.

The expectation value of $\mathcal{O}_2$ receives contributions of c_1 and c_2. $\langle\mathcal{O}_2\rangle$ is given in terms of these coefficients as

$$\langle\mathcal{O}_2\rangle = \left\langle\hat{k}\cdot(\vec{s}_1\times\vec{s}_2)\right\rangle = \frac{2\int_{-1}^{1} dz\,(z\cdot c_1 + c_2)}{4\int_{-1}^{1} dz A}. \quad (35)$$

As contributions to c_1 and c_2 are obtained by CP violating interactions, no absorptive part is required to obtain a non-zero value of $\langle\mathcal{O}_2\rangle$.

4. CP Violation in Top Quark Pair Production at the LHC in the Complex MFV-MSSM

4.1. Supersymmetric QCD Corrections at the Parton Level

The SQCD contributions to the coefficients $b_{1,CP}$, $b_{2,CP}$, c_1 and c_2 originate from vertex diagrams, top self-energies and box diagrams involving squarks and gluinos inside the loops. For these corrections the coefficients $b_{1,CP}$, $b_{2,CP}$, c_1 and c_2 factorize accordingly to

$$b_{i,CP} = g^{++}\cdot B(p_i, m_i,), \quad (36)$$

$$c_i = i\cdot g^{++}\cdot C(p_i, m_i), \quad (37)$$

where the abbreviations $B(p_i,m_i)$ and $C(p_i,m_i)$ denote some combination of tensor functions depending only on the external momenta and all occurring masses but not on particle coupling coefficients. The parameter g^{++} includes all coupling parameters (which contain all the complex phases), is purely imaginary and identical for vertex, self-energies and box diagrams. However, $g_1^{++} = -g_2^{++}$, where the index 1 stands for the case if stop quark 1 runs in the loop and the index 2 for the case if stop quark 2 runs in the loop. Therefore, the two top-squark loops will add destructively. The limits of g^{++} for the top squark index j can be obtained varying the gluino phase φ between 0 and 2π and using the unitarity of the squark mixing matrix to

$$-i\cdot 8\pi\alpha_s \;\leq\; g^{++} \;\leq\; +i\cdot 8\pi\alpha_s \quad . \tag{38}$$

It is important to note, that g^{++} is zero if no mixing is present in the top squark sector and reaches its limits for maximal mixing. From the structure of b_i in Eq. (36) and c_i in Eq. (37) it follows that $\hat{O}_1$ is only sensitive to the imaginary part of the tensor function $B(p_i,m_i)$ and $\hat{O}_2$ is only sensitive to the real part of the tensor function $C(p_i,m_i)$. In the following sections we therefore discuss the numerical dependencies of these tensor functions with respect to the masses of the supersymmetric particles and $\sqrt{\hat{s}}$. We factor out the coupling parameters and present numerical values for $Im[\hat{O}_1/g^{++}]$ and $Re[\hat{O}_2/(i\cdot g^{++})]$.

4.2. $\hat{O}_1$ and $\hat{O}_2$ as a Function of the Center of Mass energy at Parton Level

$Im[\hat{O}_1/g^{++}]$ and $Re[\hat{O}_2/(i\cdot g^{++})]$ are discussed in Fig. 1 and Fig. 2, respectively, in dependence of the partonic center of mass energy for the $q\bar{q} \to t\bar{t}$ channel. All curves have been generated for one stop quark loop only with $m_{\tilde{t}_1} = 100$ GeV and $m_{\tilde{g}} = 300$ GeV. The box contributions are summed over the squark indices 1 and 2 of the initial quark flavor q with $m_{\tilde{q}_1} = m_{\tilde{q}_2} = 500$ GeV. Fig. 1 shows that $Im[\hat{O}_1/g^{++}]$ is tiny for vertices, boxes and the total contributions until the production threshold of the resonant loop diagrams with two gluino propagators, which is reached at $\sqrt{\hat{s}} = 2m_{\tilde{g}}$. $Im[\hat{O}_1/g^{++}]$ reaches large values only for center of mass energies larger than this production threshold. On the other hand, $Re[\hat{O}_2/(i\cdot g^{++})]$ is sizeable for all $\sqrt{\hat{s}}$ above the top pair production threshold with maxima when the center of mass energy is $2m_{\tilde{g}}$. The absolute value of the maxima for the total SQCD corrections to $q\bar{q} \to t\bar{t}$ for $Im[\hat{O}_1/g^{++}]$ and $Re[\hat{O}_2/(i\cdot g^{++})]$ and the considered particle mass configuration is about 0.2 %. Eq. (38) limits g^{++} to about ± 3. The total contribution of the SQCD corrections due to one top-squark loop to the observables $\hat{O}_1$ and $\hat{O}_2$ for the $q\bar{q} \to t\bar{t}$ channel can therefore reach up to ± 0.6 %.

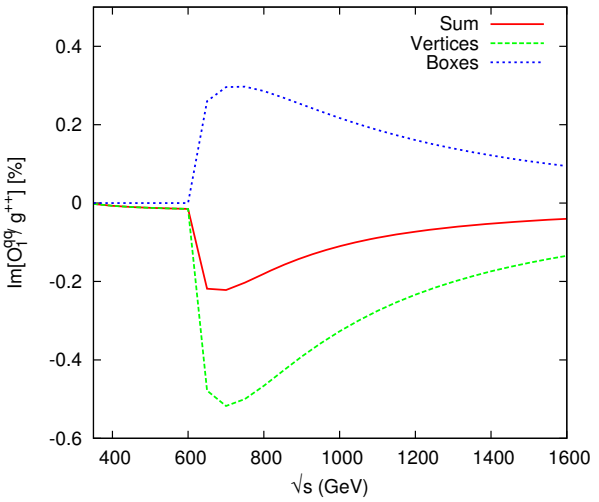

Figure 1: $q\bar{q} \to t\bar{t}$, $Im[\hat{O}_1/g^{++}]$ in % at the parton level.

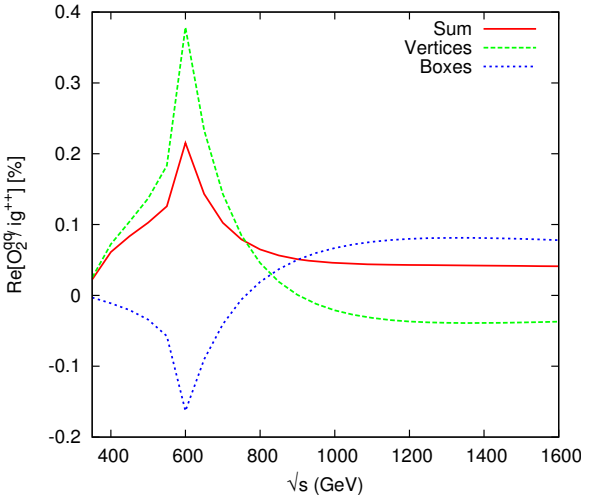

Figure 2: $q\bar{q} \to t\bar{t}$, $Re[\hat{O}_2/(i\cdot g^{++})]$ in % at the parton level.

$Im[\hat{O}_1/g^{++}]$ and $Re[\hat{O}_2/(i\cdot g^{++})]$ in dependence of $\sqrt{\hat{s}}$ for the $gg \to t\bar{t}$ channel are shown in Fig. 3 and Fig. 4, respectively. The box diagrams have been summed over the squark indices $\tilde{q}_1$ and $\tilde{q}_2$ with $m_{\tilde{q}_1} = m_{\tilde{q}_2} = 500$ GeV. All curves are shown for one stop quark only with $m_{\tilde{t}_1} = 100$ GeV and $m_{\tilde{g}} = 300$ GeV. $Im[\hat{O}_1/g^{++}]$, Fig. 3, is again tiny for the vertices, boxes and the total contribution until the production threshold of the resonant loop diagrams with two gluino propagators, which is at $2m_{\tilde{g}}$. After this threshold, the distributions reach a maxi-

mum around $\sqrt{\hat{s}} \sim 700$ GeV. The top self-energy contributions to $Im[\hat{O}_1/g^{++}]$ for the $gg \to t\bar{t}$ channel are zero for all $\sqrt{\hat{s}}$ because the corresponding loop integral is always real. $Re[\hat{O}_2/(i \cdot g^{++})]$ is non-zero for all $\sqrt{\hat{s}}$ above the top pair production threshold. The maximal contribution of the SQCD corrections for the $gg \to t\bar{t}$ channel to $Im[\hat{O}_1/g^{++}]$ is about $-0.65\,\%$ and about $-0.35\,\%$ for $Re[\hat{O}_2/(i \cdot g^{++})]$. Including the coupling limits for g^{++}, Eq. (38), the maximal contribution of the SQCD corrections for one top squark loop to the observables $\hat{O}_1$ is about $\pm 2\,\%$ and to $\hat{O}_2$ about $\pm 1\%$.

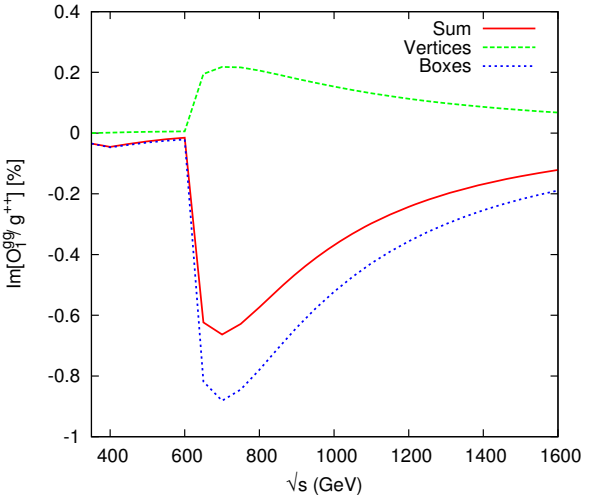

Figure 3: $gg \to t\bar{t}$, $Im[\hat{O}_1/g^{++}]$ in % at the parton level.

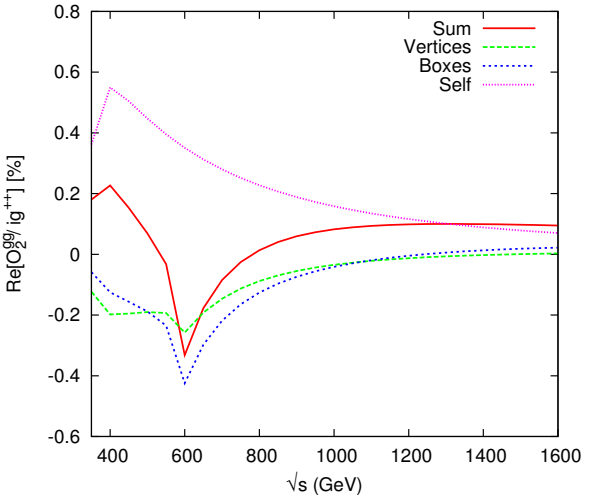

Figure 4: $gg \to t\bar{t}$, $Re[\hat{O}_2/(i \cdot g^{++})]$ in % at the parton level.

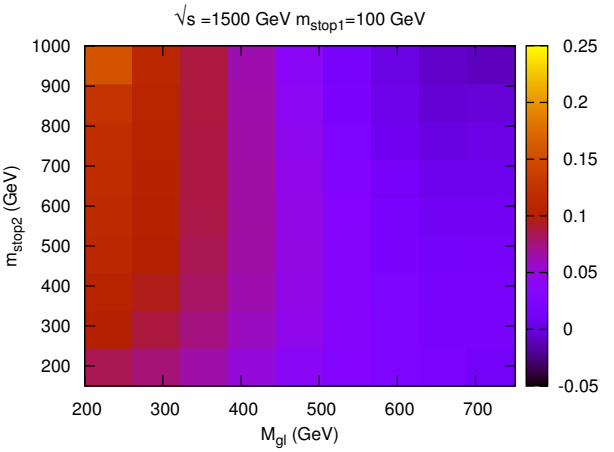

Figure 5: $gg \to t\bar{t}$, $Im[\hat{O}_1/g_1^{++}]$ in %, summed over both top squark loops.

4.3. $\hat{O}_1$ and $\hat{O}_2$ as a Function of Stop and Gluino Masses at Parton Level

In this section we show for the example of the $gg \to t\bar{t}$ channel, $Im[\hat{O}_1/g_1^{++}]$ and $Re[\hat{O}_2/g_1^{++}]$ in dependence of the stop1, stop2 mass splitting and the gluino mass. We sum the contribution of the loops with a top-squark 1 and with a top-squark 2 and factor out the coupling parameter factor g_1^{++} of the top squark 1. As mentioned above, the resulting loop contributions of the two squark loops will be independent of coupling parameters but add destructively.

Fig. 5 shows $Im[\hat{O}_1/g_1^{++}]$ in dependence of the gluino mass and the heavier top-squark mass (stop2). We fix the partonic center of mass energy to 1500 GeV and the lighter top squark mass (stop1) to 100 GeV. Fig. 5 shows, that $Im[\hat{O}_1/g_1^{++}]$ reaches its largest values of $\sim 0.25\%$ for light gluino masses between 200 and 300 GeV and a large $m_{\tilde{t}_2}$ of 1000 GeV, corresponding to a large $m_{\tilde{t}_1}$ - $m_{\tilde{t}_2}$ mass splitting. $Im[\hat{O}_1/g_1^{++}]$ decreases if the top-squark mass splitting decreases. If the gluino mass increases to $500 - 600$ GeV the contribution to $Im[\hat{O}_1/g_1^{++}]$ vanishes to zero and obtains negative values of $\sim -0.1\%$ in regions with gluino masses between $600 - 750$ GeV and stop2 masses around $800 - 1000$ GeV.

Fig. 6 shows $Re[\hat{O}_2/g_1^{++}]$ for the $gg \to t\bar{t}$ channel with $\sqrt{\hat{s}} = 1500$ GeV and $m_{\tilde{t}_1} = 100$ GeV. $Re[\hat{O}_2/g_1^{++}]$ is largest with $\sim 0.15 - 0.2\%$ for small gluino masses of $200 - 300$ GeV and large $m_{\tilde{t}_1}$ - $m_{\tilde{t}_2}$ mass splitting. Also here, $Re[\hat{O}_2/g_1^{++}]$ decreases if the top-squark mass splitting decreases. For larger gluino masses,

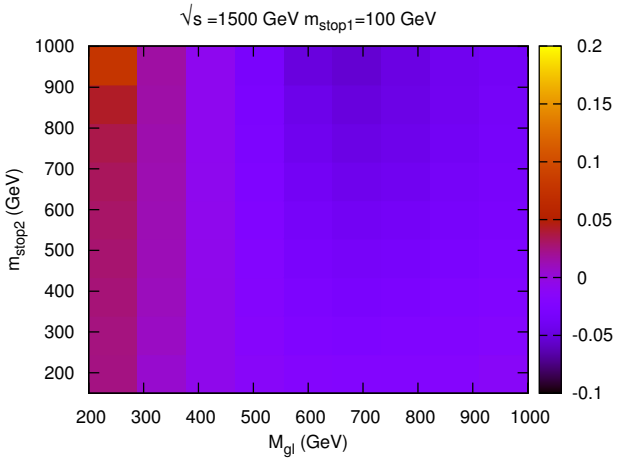

Figure 6: $gg \to t\bar{t}$, $Re[\hat{O}_2/(i \cdot g_1^{++})]$ in %, summed over both top squark loops.

the contribution to $Re[\hat{O}_2/g_1^{++}]$ quickly goes to zero and becomes negative $\sim -0.05\%$ for gluino masses between $550 - 800$ GeV and a large $m_{\tilde{t}_1}$ - $m_{\tilde{t}_2}$ mass splitting. The contributions drop to zero for mass-degenerated top-squarks.

The above results show that CP violating effects of SQCD corrections at the parton level for both observables $\hat{O}_1$ and $\hat{O}_2$ can be of the order of a percent for very light gluino masses of $200 - 300$ GeV and of the order of per mille for heavier gluino masses. Furthermore, the contributions are the larger, the larger the splitting between the stop masses.

5. Conclusions

We investigated possible CP violating effects in top pair quark production at the LHC, which arise at the one loop level due to possible complex phases of the MFV-MSSM. We included the complete supersymmetric QCD as well as supersymmetric electroweak contributions to the quark-antiquark annihilation, $q\bar{q} \to t\bar{t}$, and gluon fusion, $gg \to t\bar{t}$. At the level of the top quarks, we studied in detail two observables that are sensitive to such complex phases, $\langle \mathcal{O}_1 \rangle$ and $\langle \mathcal{O}_2 \rangle$.

We presented results for these observables at the parton level and determined their maximal correction due to supersymmetric particles. The SQCD corrections are at least an order of magnitude larger than SEW corrections. We found that gluon fusion dominates the asymmetries and that they are largest for small invariant masses of the top quark pair. To summarize, the result of this work suggests interesting CP violating effects which may arise due to SQCD corrections to gluon fusion in top quark pair production and thus warrant further, more detailed studies which are in progress [17].

References

[1] W. Bernreuther, Top quark physics at the LHC, J.Phys. G35 (2008) 083001. arXiv:0805.1333, doi:10.1088/0954-3899/35/8/083001.

[2] D. Wackeroth, Top quark theory review for the Tevatron, LHC, and ILCarXiv:0810.4176.

[3] V. Abazov, et al., First measurement of the forward-backward charge asymmetry in top quark pair production, Phys.Rev.Lett. 100 (2008) 142002. arXiv:0712.0851, doi:10.1103/PhysRevLett.100.142002.

[4] C. Kao, D. Wackeroth, Parity violating asymmetries in top pair production at hadron colliders, Phys.Rev. D61 (2000) 055009. arXiv:hep-ph/9902202, doi:10.1103/PhysRevD.61.055009.

[5] T. Stelzer, S. Willenbrock, Spin correlation in top quark production at hadron colliders, Phys.Lett. B374 (1996) 169–172. arXiv:hep-ph/9512292, doi:10.1016/0370-2693(96)00178-5.

[6] A. Brandenburg, Spin spin correlations of top quark pairs at hadron colliders, Phys.Lett. B388 (1996) 626–632. arXiv:hep-ph/9603333, doi:10.1016/S0370-2693(96)01347-0.

[7] G. Mahlon, S. J. Parke, Maximizing spin correlations in top quark pair production at the tevatron, Phys. Lett. B411 (1997) 173–179. arXiv:hep-ph/9706304.

[8] A. Brandenburg, M. Maniatis, SUSY QCD corrections to the polarization and spin correlations of top quarks produced in e+ e- collisions, Phys.Lett. B558 (2003) 79–91. arXiv:hep-ph/0301142, doi:10.1016/S0370-2693(03)00210-7.

[9] K. Melnikov, M. Schulze, Top quark spin correlations at the Tevatron and the LHC, Phys.Lett. B700 (2011) 17–20. arXiv:1103.2122, doi:10.1016/j.physletb.2011.04.043.

[10] S. J. Parke, Top Quark Spin Correlations - Theory, Nuovo Cim. C035N3 (2012) 111–114. arXiv:1202.2345, doi:10.1393/ncc/i2012-11229-2.

[11] J. Wess, B. Zumino, A Lagrangian Model Invariant Under Supergauge Transformations, Phys.Lett. B49 (1974) 52. doi:10.1016/0370-2693(74)90578-4.

[12] J. Wess, B. Zumino, Supergauge Transformations in Four-Dimensions, Nucl.Phys. B70 (1974) 39–50. doi:10.1016/0550-3213(74)90355-1.

[13] A. Buras, P. Gambino, M. Gorbahn, S. Jager, L. Silvestrini, Universal unitarity triangle and physics beyond the standard model, Phys.Lett. B500 (2001) 161–167. arXiv:hep-ph/0007085, doi:10.1016/S0370-2693(01)00061-2.

[14] G. D'Ambrosio, G. Giudice, G. Isidori, A. Strumia, Minimal flavor violation: An Effective field theory approach, Nucl.Phys. B645 (2002) 155–187. arXiv:hep-ph/0207036, doi:10.1016/S0550-3213(02)00836-2.

[15] M. Frank, T. Hahn, S. Heinemeyer, W. Hollik, H. Rzehak, et al., The Higgs Boson Masses and Mixings of the Complex MSSM in the Feynman-Diagrammatic Approach, JHEP 0702 (2007) 047. arXiv:hep-ph/0611326, doi:10.1088/1126-6708/2007/02/047.

[16] W. Bernreuther, A. Brandenburg, Tracing CP violation in the production of top quark pairs by multiple TeV proton proton collisions, Phys.Rev. D49 (1994) 4481–4492. arXiv:hep-ph/9312210, doi:10.1103/PhysRevD.49.4481.

[17] S. Berge, M. Muehlleitner, A. Moreno Briceño, D. Wackeroth, M. Wiebusch, in preparation.